CrystEngComm

Accepted Manuscript

ROYAL SOCIETY OF CHEMISTRY

www.rsc.org/crystengcomm

Journal Name

RSCPublishing

ARTICLE

Hydrated anion glued capsular and non-capsular assembly of a tripodal host: solid state recognition of bromide-water $[Br_5\text{-}(H_2O)_6]^{5-}$ and iodide-water $[I_2\text{-}(H_2O)_4]^{2-}$ clusters in cationic tripodal receptor

Cite this: DOI: 10.1039/x0xx00000x

Received 00th January 2012,
Accepted 00th January 2012

DOI: 10.1039/x0xx00000x

www.rsc.org/

Md. Najbul Hoque[a] and Gopal Das*[a]

ABSTRACT: Herein, we have described a flexible polyammonium tripodal (N4 unit) receptor for hydrated anions. Multiple protonation sites increased the degree of pronation and allowed to study binding of multiple anions towards the receptor in aqueous medium. All three arms are projected in the same direction in the protonated receptor and formed bowl shaped conformation. Whereas the free receptor **L** occupied an orientation in between open and bowl shaped conformation. We observed anion or anion-water assisted capsular and non-capsular assembled supramolecular structures and stabilized by several H-bonding interactions. We have shown fluoride-water and chloride ion belt induced bimolecular capsular assemblies in complexes **1** and **3**. On the other hand, we have established chloride-water, bromide-water and iodide-water templated non-capsular aggregations of the protonated receptor in complexes **2**, **4** and **5**. Most interestingly, a long chain fluoride-water cluster $[F_7\text{-}(H_2O)_8]^{7-}$ in capsular complex **1**, unique extended bromide-water $[Br_5\text{-}(H_2O)_6]^{5-}$ and discrete iodide-water $[I_2\text{-}(H_2O)_4]^{2-}$ clusters in non-capsular complexes **4** and **5** are also examined structurally. All supramolecular complexes are characterized by FTIR, NMR, TGA-DSC and X-ray analysis.

Introduction

Since decades it is well known the role of inorganic anions in biological, atmospheric, environmental chemistry.[1] Aqueous solvation of inorganic anions is highly active area for understanding their structures, activities and energetics in solvated state.[2] The random orientation of molecules in aqueous network that results hydrated anions is very complex due to strong stability of H-bonding interaction. The behaviors of hydrated anions are interestingly different from those of free anions or anions in non-polar media as its reactivity largely depends on surrounding hydration networks and molecular hosts. Therefore, a molecular level perspective of ordered anion-water cluster in synthetic receptor allows us to explore the molecular interaction of anions with water moecules.[3]

Halide ions are ubiquitous and plays diverse role in nature and physiology.[4] For example hydration of fluoride ion is interesting due to its smaller size and high electronegativity.[5] In reality it remains in strongly hydrated form due to its high hydration enthalpy. So consumption of fluoride containing drinking water is a concerning matter as its high level causes skeletal and dental fluorosis.[6] An important aspect of chloride ion in CIC (Charcot Leyden crystal) channels in transportation of chloride ion across cellular membrane is well established.[7] Another halide ion iodide remains dissolved in sea water and believed to be main source of iodide ions in atmosphere which increases ozone level in upper atmosphere.[8] Apart from that study of iodide-water cluster have been emphasized due to high polarizability and large ionic radii of iodide ion.[9] Hence study of hydrated anions in terms of solvation and recognition is of great importance. As a result in the past decades care full attention have been given in recognition of hydrated anions in polar or non-polar medium by several synthetic receptors containing multiple anions like $[F_2\text{-}(H_2O)_6]^{2-}$,[10] $[F_4\text{-}(H_2O)_{10}]^{4-}$,[11] $[F\text{-}(H_2O)]_4^{4-}$,[12] $[Cl\text{-}(H_2O)_4]^{-}$,[13] $[Cl_2\text{-}(H_2O)_2]^{2-}$,[14] $[Cl_2\text{-}(H_2O)_4]^{2-}$,[15] $[Cl_2\text{-}(H_2O)_6]^{2-}$,[16] $[Cl_3\text{-}(H_2O)_4]^{3-}$,[17] $[Br_2\text{-}(H_2O)_2]^{2-}$,[14] $[Br_2\text{-}(H_2O)_6]^{2-}$[18] and $[I_2\text{-}(H_2O)_6]^{2-}$.[19] It is worth to mention that anion-water cluster mediated assembly has been less extensively studied with few exceptions of halide-water cluster mediated supramolecular capsules.[10,11,14,15] So in this direction anion-water induced assembly process is particularly a new window and can provide much more informations about the behavior of hydrated anions in various supramolecular systems. In our continuing study on anion-water clusters and their role in formation of supramolecular architectures,[14,17,20] herein, we present capsular and non-capsular assembly of polyammonium based tripodal receptor triggered by anion or anion-water cluster. In addition we report fluoride-water chain $[F_7\text{-}(H_2O)_8]^{7-}$, an unique formation of bromide-water $[Br_5\text{-}(H_2O)_6]^{5-}$ cluster containing chair like bromide-water hexamer and iodide-water $[I_2\text{-}(H_2O)_6]^{2-}$ clusters consisting water tetramer in cationic tripodal receptor.

Experimental section

Materials and Methods

^{1}H and ^{13}C NMR spectra were recorded on a Varian FT-400 MHz spectrometer in CD_3OD or D_2O at 298 K. The IR spectra were recorded on a Perkin-Elmer-Spectrum One FT-IR spectrometer with KBr disks in the range 4000-500 cm^{-1}. The starting materials triethanol amine, thionyl chloride and *p*-nitrophenol were purchased from Sigma-Aldrich, USA and were used as received and tris[2-(4-nitrophenoxy)ethyl]amine was prepared according to our previously reported procedure.[21] Solvents were purchased from Spectrochem Ltd., India. Chemical shifts for ^{1}H and ^{13}C NMR were reported in parts per million (ppm), calibrated to the residual solvent peak set. Thermogravimetric analysis (TGA) and differential scanning calorimetry (DSC) were performed on a TA Instruments Q20 differential scanning calorimeter and SDT Q600 analyzer under nitrogen atmosphere with a heating rate of 7 °C.

Crystallographic Refinement Details

The crystallographic data and details of data collection for free receptor **L** and complexes **1**, **2**, **3**, **4** and **5** are given in Table S1. In each case, a crystal of suitable size was selected from the mother liquor and immersed into silicone oil, then mounted on the tip of a glass fiber and cemented using epoxy resin. Intensity data for the all crystals were collected Mo-Kα radiation (λ = 0.71073Å) at 298(2) K, with increasing ω (width of 0.3° per frame) at a scan speed of 6 s/ frame on a Bruker SMART APEX diffractometer equipped with CCD area detector. The data integration and reduction were processed with SAINT[22a] software. An empirical absorption correction was applied to the collected reflections with SADABS.[22b] The structures were solved by direct methods using SHELXTL[22c] and were refined on F^2 by the full-matrix least-squares technique using the SHELXL-97 program package.[22d] Graphics are generated using MERCURY 3.0.[22e] In all cases, non-hydrogen atoms are treated anisotropically. The hydrogen atoms are located on a difference Fourier map and refined. In other cases, the hydrogen atoms are geometrically fixed. It is important to mention that we could not locate H-atom in logical senses on water molecule (O6w) in chloride complex **2** and bromide complex **4** and O8w, O9w in iodide complex **5**.

Synthesis and characterization

Preparation of tris[2-(4-aminophenoxy)ethyl]amine (L)

The tripodal receptor **L** was prepared by following procedure. Yellow crystalline tris[2-(4-nitrophenoxy)ethyl]amine (1.0 g) was taken into RB containing 50 ml ethanol and heated for 1 hr to dissolve the crystals. The solution was allowed to reach room temperature and to this solution 2 mL hydrazine and 0.02 g Pd/C was added and finally the whole mixture was refluxed at 80 °C for another 24 hrs for the completion of the reaction. The Pd/C was filtered off and the filtrate was kept into beaker which afforded the colorless crystals of tripodal amine **L** within 24 hrs (Scheme 1, ESI).

Receptor **L**: Yield = 95%, M. P: 141-143 °C. ^{1}H-NMR (600 MHz, CD_3OD) δ (ppm): 6.668 (d, J = 6.2 Hz, 2H, C—H_{ar}), 6.630 (d, J = 6.0 Hz, 2H, C—H_{ar}), 4.510 (s, 2H, –NH_2), 3.972 (t, J = 5.4 Hz, 2H, C—H_{alp}), 3.004 (t, J = 6.0 Hz, 2H, C—H_{alp}). ^{13}C-NMR (150 MHz, CD_3OD) δ (ppm): 153.57, 142.07, 118.36, 116.94, 68.51 and 55.72. IR spectra (KBr pellet): 3430 cm^{-1} *vs*(N—H), 3350 cm^{-1} *vs*(N—H), 2972 cm^{-1} (C—H_{ar}), 2916 cm^{-1} (C—H_{alp}), 1620 cm^{-1} *vb*(N—H), 1518 cm^{-1} *vs*(C=C), 1222 cm^{-1}, 824 cm^{-1}.

Preparation of different salts

[**L**H_4·4F·5H_2O](**1**)**:** To a 1 ml water of **L** in a small plastic container (0.052 g, 0.125 mmol) was added 1-2 drops of hydrofluoric acid (HF) and stirred for 1 hr to obtain a clear solution. Finally the aqueous mixture kept for crystallization in open atmosphere. After rapid evaporation it afforded colorless X-ray mountable single crystal just within a day.

Complex **1**: Yield = 90%, M. P: 175-177 °C. ^{1}H-NMR (600 MHz, CD_3OD:D_2O, 1:2) δ (ppm): 7.401 (d, J = 6.6 Hz, 2H, C—H_{ar}), 7.142 (d, J = 6.6 Hz, 2H, C—H_{ar}), 4.578 (t, J = 4.2 Hz, 2H, C—H_{alp}), 4.011 (t, J = 4.2 Hz, 2H, C—H_{alp}). IR spectra (KBr pellet): broad and sharp band at 3435 cm^{-1} *vs*(N—H and O—H), 3140 cm^{-1} *vs*(N—H), broad band at 2875 cm^{-1} (N—H), 2590 cm^{-1} (C—H), 1620 cm^{-1} *vb*(N—H), 1510 cm^{-1} *vs*(C=C), 1259 cm^{-1}, 1222 cm^{-1}, 833 cm^{-1}, 740 cm^{-1}.

[2**L**H_4·8Cl·5H_2O](**2**)**:** To a 1 ml water of **L** in a small beaker (0.052 g, 0.125 mmol) was added 1-2 drops of hydrochloric acid (HCl) and stirred for 1 hr to obtain a clear solution. Finally the aqueous mixture kept for crystallization in open atmosphere. After rapid evaporation it afforded colorless X-ray mountable single crystal just within a day.

Complex **2**: Yield = 90%, M. P: 238-240 °C. ^{1}H-NMR (600 MHz, CD_3OD:D_2O, 1:2) δ (ppm): 7.319 (d, J = 8.4 Hz, 2H, C—H_{ar}), 7.021 (d, J = 8.4 Hz, 2H, C—H_{ar}), 4.492 (t, J = 4.6 Hz, 2H, C—H_{alp}), 3.938 (t, J = 4.8 Hz, 2H, C—H_{alp}). IR spectra (KBr pellet): broad band at 3440 cm^{-1} *vs*(N—H and O—H), 3150 cm^{-1} *vs*(N—H), broad band 2882 cm^{-1} (N—H), 2580 cm^{-1} (C—H), 1611 cm^{-1} *vb*(N—H), 1510 cm^{-1} *vs*(C=C), 1259 cm^{-1}, 833 cm^{-1}.

[**L**H_4·4Cl](**3**): To a 1 ml DMF of **L** in a glass vial (0.052 g, 0.125 mmol) was added 1-2 drops of HCl acid and stirred for 1 hr. Finally glass vial kept for crystallization in open atmosphere. It afforded colorless X-ray mountable single crystal after 1-2 weeks.

Complex **3**: Yield = 70%, M. P: 255-256 °C. ^{1}H-NMR (600 MHz, CD_3OD:D_2O, 1:2) δ (ppm): 7.367 (d, J = 9.0 Hz, 2H, C—H_{ar}), 7.069 (d, J = 9.0 Hz, 2H, C—H_{ar}), 4.545 (t, J = 3.6 Hz, 2H, C—H_{alp}), 3.985 (t, J = 3.6 Hz, 2H, C—H_{alp}). IR spectra (KBr pellet): broad band at 3440 cm^{-1} *vs*(N—H and O—H), 3150 cm^{-1} *vs*(N—H), broad band at 2882 cm^{-1} (N—H), 2580 cm^{-1} (C—H), 1611 cm^{-1} *vb*(N—H), 1510 cm^{-1} *vs*(C=C), 1259 cm^{-1}, 833 cm^{-1}.

[**L**H_4·4Br·5H_2O](**4**): To a 1 ml water of **L** in a small beaker (0.052 g, 0.125 mmol) was added 1-2 drops hydrobromic acid (HBr) and stirred for 1 hr to obtain a clear solution. Finally the aqueous mixture kept for crystallization in open atmosphere. After rapid evaporation it afforded colorless X-ray mountable single crystal just within a day.

Complex **4**: Yield = 85%, M. P: 282-284 °C. ^{1}H-NMR (600 MHz, CD_3OD:D_2O, 1:2) δ (ppm): 7.401 (d, J = 6.6 Hz, 2H, C—H_{ar}), 7.142 (d, J = 6.6 Hz, 2H, C—H_{ar}), 4.578 (t, J = 4.2 Hz, 2H, C—H_{alp}), 4.011 (t, J = 4.2 Hz, 2H, C—H_{alp}). IR spectra (KBr pellet): broad band at 3435 cm^{-1} *vs*(N—H and O—H), 3145 cm^{-1} *vs*(N—H), broad band at 2882 cm^{-1} (N—H), 2585 cm^{-1} (C—H), 1611 cm^{-1} *vb*(N—H), 1510 cm^{-1} *vs*(C=C), 1259 cm^{-1}, 833 cm^{-1}.

[4**L**H_4·16I·7H_2O](**5**). To a 1 ml water of **L** in a small beaker (0.052 g, 0.125 mmol) was added 1-2 drops hydriodic acid (HI) and stirred for 1 hr to obtain a clear solution. Finally the aqueous mixture kept for crystallization in open atmosphere. After rapid evaporation it afforded colorless X-ray mountable single crystal within a day.

Complex **5**: Yield = 80%, M. P: 288-289 °C. ^{1}H-NMR (600 MHz, CD_3OD:D_2O, 1:2) δ (ppm): 7.355 (d, J = 7.5 Hz, 2H,

Table 1 Crystallographic data and refinement details for compounds **1-6**

Code name	**L**	Complex **1**	Complex **2**	Complex **3**	Complex **4**	Complex **5**
Empirical formula	$C_{24}H_{30}N_4O_3$	$C_{24}H_{44}F_4N_4O_8$	$C_{48}H_{78}Cl_8N_8O_{11}$	$C_{24}H_{34}Cl_4N_4O_3$	$C_{24}H_{44}Br_4N_4O_8$	$C_{96}H_{150}I_{16}N_{16}O_{19}$
Formula weight	422.52	592.63	1224.77	568.35	836.22	3862.67
Crystal system	Hexagonal	Monoclinic	Triclinic	Hexagonal	Monoclinic	Triclinic
a (Å)	19.2271(4)	23.2013(12)	11.4963(6)	12.7399(8)	12.6464(4)	12.6814(6)
b (Å)	19.2271(4)	11.1503(4)	12.2339(6)	12.7399(8)	11.5355(4)	13.0383(6)
c (Å)	10.2751(2)	24.7773(10)	13.0811(8)	62.0390(5)	24.2735(8)	20.9938(10)
α (degree)	90.00	90.00	111.373(5)	90.00	90.00	75.377(2)
β (degree)	90.00	114.561(6)	113.194(5)	90.00	104.935(2)	87.245(2)
γ (degree)	120.00	90.00	94.457(4)	120.00	90.00	88.453(2)
V (Å^3)	3289.61(12)	5830.00(5)	1521.28(14)	8720.20(10)	3421.50(2)	3354.50(3)
space group	*R3c*	*C2/c*	*P-1*	*R-3c*	$P2_1/c$	*P -1*
Z value	6	8	1	12	4	1
ρ(cal)(g/cm^3)	1.280	1.350	1.337	1.229	1.621	1.909
μ(Mo Kα) (mm^{-1})	0.086	0.116	0.430	0.438	4.751	3.750
T(K)	298(2)	298(2)	298(2)	298(2)	298(2)	298(2)
R1; wR2 (I> 2 σ(I))	0.0349; 0.1059	0.0780; 0.2311	0.0492; 0.1656	0.0478; 0.1313	0.0353; 0.1029	0.0677; 0.1751
R1; wR2(all)	0.0379; 0.1095	0.1039; 0.2563	0.0682; 0.2006	0.0715; 0.1497	0.0545; 0.1205	0.0965; 0.1946
Residual electron density	0.122/-0.170	0.783/-0.364	0.604/-0.537	0.548/-0.172	0.451/-0.638	3.107/-3.423
good-of-fit	0.906	0.980	0.690	1.004	0.910	1.112
Reflection measured	16238	13715	11469	12681	30309	14556
Unique reflns	1799	4624	5194	2527	6895	8849
Reflection parameters	94	391	365	110	404	694
CCDC No.	961078	961079	961081	961080	961082	978948

C—H_{ar}), 7.098 (d, *J* = 7.3 Hz, 2H, C—H_{ar}), 4.541 (t, *J* = 4.3 Hz, 2H, C—H_{alp}), 4.980 (t, *J* = 4.5 Hz, 2H, C—H_{alp}). IR spectra (KBr pellet): broad band at 3420 cm^{-1} *vs*(N—H and O—H), 3138 cm^{-1} *vs*(N—H), broad 2879 cm^{-1} (N—H), 2550 cm^{-1} (C—H), 1611 cm^{-1} *vb*(N—H), 1509 cm^{-1} *vs*(C=C), 1268 cm^{-1}, 824 cm^{-1}.

Results and discussion

The big advantages of polyammonium based anion receptors are high degree of protonation that enhance the possibility of binding of multiple anions. The solubility of such protonated receptors in protic solvent open the scope for the study of solvation properties of anions and anion-water interactions in highly polar medium in confined systems which is very relevant to realistic phenomenon. We have designed very important and new receptor considering the same plat form of having apical nitrogen atom and three amine groups forming a N_4 unit. Another famous N_4 unit (tren based receptor) has widely been studied where apical nitrogen atom does not get protonated.[23c] But in our case proper decoration by placing of ethereal function in the tripodal amine helps for the protonation of the apical nitrogen and allow the binding of multiple anions in protic solvent. The interesting outcome of this report is that we are able to isolate anion or anion-water assisted capsular and non-capsular supramolecular assembly and most significantly anion-water clusters by tripodal receptor in aqueous medium.

Structural study of free receptor L

The free receptor **L** was crystallized during evaporation of the ethanolic solution within 24 hrs. Structural study obtained from single crystal X-ray shows that **L** crystallizes in highly symmetric hexagonal *R3c* space group. Solid state structure indicates the asymmetric unit contains only the receptor and a C_{3v} axis passes through the apical N-atom. The average bond distance between apical nitrogen and adjacent carbon in free receptor (N—C) is 1.477 Å. The ethereal separation (O···O = 4.798 Å) of three identical oxygen atom and torsion angle value (N_{apical}–C–C–O_{ether} = 81.1°) suggest that receptor adopted an orientation in between folded and open conformation[23] as depicted in Fig. 1a. Interaction pattern shows all three ethereal oxygen form highly directed C_{ar}—H···O (C5···O1 = 3.536(2) Å) H-bond. All three —NH_2 groups are involved in H-bonding with aliphatic CH_2, phenyl ring with distances N2···C2 = 3.611(3) Å and C8···N2 = 3.593(2) Å respectively (Table S1). The receptor is stabilized by all these weak interactions in solid state. Close inspection in the crystal packing indicates that each tripodal unit is surrounded by six neighbored tripodal units that form a cyclohexane like highly symmetric hexagonal structure which is highlighted in Fig. 1b. There are three aliphatic C—H···π interactions (C2···Cg = 3.811 Å) between two tripodal unit that generate sheet structure of the tripodal. IR spectra of free receptor **L** showed two sharp bands at 3430 cm^{-1} and 3350 cm^{-1} for N—H stretching frequency. Experimental and simulated PXRD pattern of free receptor **L** confirmed the bulk phase purity.

Structural Study of Halide Complexes of L

Structural Study of Complex [LH_4·4F·5H_2O](1)

Single crystal X-ray study of the complex [LH_4·4F·5H_2O]**(1)** shows it crystallizes in monoclinic system with centrosymmetric space group *C2/c*. The asymmetric unit contains one protonated receptor [LH_4]$^{4+}$, four fluoride ions and five water of crystallization. The protonated receptor contains a

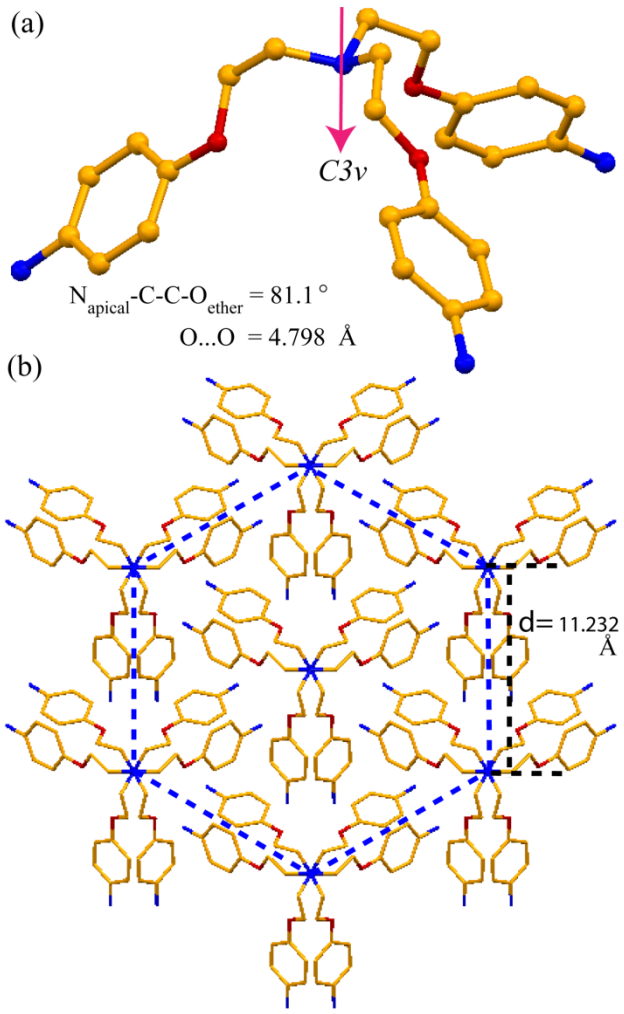

Fig. 1 (a) Crystal structure of **L** showing an orientation neither in a folded nor in an open conformation and a C_{3v} axis of symmetry passing through apical N-atom. (b) Hexagonal arrangement of tripodal pair along *c*-axis showing cyclohexane like structure as a result of C—H···π and C—H···O interactions.

C_{3v} axis passing through apical N-atom and fluoride ion (F1). Crystal structure shows that all four nitrogen atoms of the tripodal receptor are protonated and produced tetra fluorinated highly ionic environment. Protonation on apical N-atom in fluoride complex **1** is further confirmed by the bond distance between apical N-atom and adjacent carbon (N—C) increased to 1.507 Å as observed in literature for apical nitrogen protonated receptors.[23] The hydrogen on apical nitrogen is directed towards the cavity and interacts with three ethereal oxygen atom in trifurcated fashion (average N1···O = 2.744 Å) that instigate the locks up conformation by decreasing the size of the cavity compared to free receptor **L** (Fig. S20a). With the formation of trifurcated H-bond, the concomitant decrease in ethereal bond distance (average O···O = 3.529 Å) and torsion angle (average N_{apical}–C–C–O_{ether} = 60°) also support the organization of three arms in the same direction and formation of bowl shaped cavity. In protonated form three phenyl rings are orthogonal each other and as a consequence we observed three intramolecular C—H_{ar}···π interactions among three tripodal arms. Three ammonium groups, the main H-bonding part of the receptor acts as a donor toward water and fluoride ion, interacts with total four water molecules and five fluoride ions. Structural analysis shows three hydrogen of $[N(2)H_3]^+$ interacts with one fluoride ion (F2) and two water molecules (O5w and O8w) having bond length N2···F2 = 2.680(5) Å, N2···O5w = 2.734(6) Å and N2···O8w = 2.606(6) Å. Whereas three hydrogen of $[N(3)H_3]^+$ interacts with two fluoride ions F3, F5 and one water molecule O4w *via* strong N3···F3 = 2.691(3) Å, N3···F5 = 2.603(3) Å and N3···O4w = 2.828(4) Å H-bonds. The other $[N(4)H_3]^+$ also forms three H-bonds with two fluoride ions (F2, F5) and one water molecule (O7w) having close contacts N4···F2 = 2.766(5) Å, N4···F5 = 2.683(4) Å and N4···O7w = 2.767(5) Å (Fig. S20b). Very interestingly complex **1** in the solid state form bimolecular capsule by association of two $[LH_4]^{4+}$ unit *via* these H-bonding interactions and stitched by fluoride-water cluster depicted in Fig. 2a. A top view shown in Fig. 2b describes the formation of fluoride-water belt in the bimolecular capsule. One fluoride ion (F1) perfectly buried at the center of the bimolecular capsule and interacts with two neighbouring water molecules (O5w). The capsule is built mainly from H-bonding interactions of $[NH_3]^+$ groups with fluoride ions and water molecules. Close up view of fluoride-water belt and several H-bonding interactions involved in the capsule are shown in Fig. 2c. The distance between two apical N-atoms in the bimolecular capsular is 17.157 Å. It is evident from the Fig. 2d that each bimolecular capsule interacts with the neighbour capsule which is accompanied by several strong and weak H-bonding interactions arising from fluoride ions and water molecules. This would actually lead the formation of supramolecular structure made of the protonated tripodal receptor. Close inspection shows two capsules are assembled by fluoride-water cluster and with the help of $[NH_3]^+$ group it actually resulted the structural motif consisting of $[F^-$-H_2O-$NH_3^+]$ backbone. A backbone of $[F^-$-H_2O-$NH_3^+]$ motif having fused hexameric (one) and pentameric ring (two) gave $[F_4$-$(H_2O)_4$-$(NH_3)_4]$ twelve membered cyclic motif existing between two capsules. The startling feature in the crystal structure of complex **1** is the formation of a long fluoride-water chain $[F_7$-$(H_2O)_8]^{7-}$ which is highlighted in Fig. 2e. The chain is mainly stabilized by strong O···F, N···O and N···F H-bonding interactions. The chain contains a mirror plane passing through F1. Further aromatic hydrogen C—H_{ar}···F and aliphatic hydrogen C—H_{alp}···F, C—H_{alp}···O also takes part in weak interactions and plays a crucial role to grow supramolecular assembly. Crystal packing along *b*-axis shows $[LH_4]^{4+}$ unit form cationic bilayer and surrounded by fluoride-water hydrophilic channel (Fig. S20c). All H-bonding details are given in Table S1. IR spectra of complex **1** exhibit a peak at 3435 cm^{-1} expected for water molecule in crystal lattice (Fig. S9). The comparable simulated and experimental PXRD pattern suggested to the bulk phase purity of the crystalline complex (Fig. S15).

Structural Study of Complex $[2LH_4{\cdot}8Cl{\cdot}5H_2O](2)$

Crystallographic analysis reveals that complex **2** crystallizes in triclinic *P-1* space group with an asymmetric unit containing one independent tetra-protonated receptor $[\mathbf{L}H_4]^{4+}$, four chloride ions and three water molecules. The receptor possesses a C_{3v} symmetry axis passing through apical N-atom. In solid state structure we observed, half part (green) is related to other half by forming an inversion center through the water molecule (O6w) giving molecular structure $[2\mathbf{L}H_4{\cdot}8Cl{\cdot}5H_2O]$ showed in Fig. 3a. The N—C bond distance (1.503 Å) in complex **2** is also parallel as observed for protonated receptor (apical N-atom). The proton on apical N-atom is directed towards the cavity and holds three arms in the same direction by forming H-bond with three ethereal oxygen atoms (average N1···O = 2.741 Å,

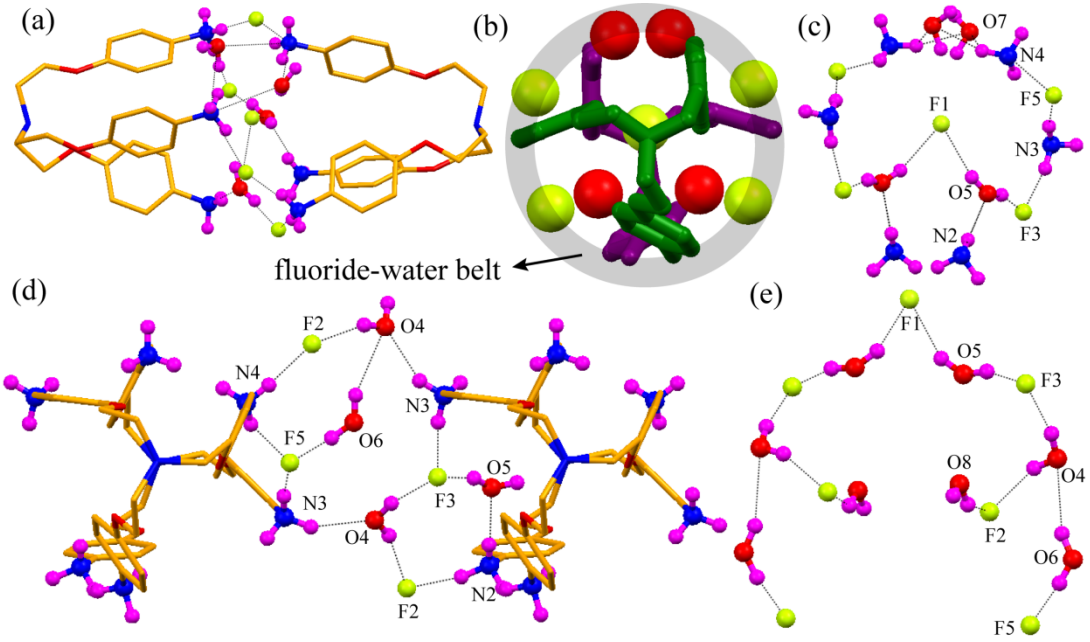

Fig. 2 (a) Side view showing fluoride-water stitched bimolecular capsular aggregate of cationic receptor $[LH_4]^{4+}$ in complex **1**. (b) Top view explaining the bimolecular molecular capsule stitched by fluoride-water belt and encapsulation of one fluoride ion. (c) Partial structure showing the H-bonding involved in fluoride-water belt in the bimolecular capsule. (d) View showing interaction between two capsules mediated by fluoride-water. (e) Picture depicting the longest fluoride-water chain $[F_7(H_2O)_8]^{7-}$ observed in solid state structure of complex **1**. H-atoms omitted from the pictures for clarity.

Fig. S21a). Ethereal bond distance (O···O = 3.563 Å) and torsion angle value (N_{apical}–C–C–O_{ether} = 60°) is comparable with complex **1** which is in good agreement for folded conformation. The orthogonal C—H···π interactions among phenyl rings are also additive force in the formation of folded conformation. In solid state all three $[NH_3]^+$ groups interacts with water molecules and chloride ions by virtue of its donor ability explained in Fig. 3b. The $[N(2)H_3]^+$ donates all three hydrogen to three chloride ions through N2···Cl1 = 3.174(3) Å, N2···Cl2 = 3.072(4) Å and N2···Cl3 = 3.204(4) Å interactions. H-bonding mode of $[N(3)H_3]^+$ is similar with that of $[N(2)H_3]^+$ containing distances N3···Cl1 = 3.163(4) Å, N3···Cl3 = 3.225(3) Å and N3···Cl4 = 3.160(3) Å. Whereas the third ammonium group $[N(4)H_3]^+$ is surrounded by two chloride ions and one water molecule with H-bond distances N4···Cl3 = 3.218(3) Å, N4···Cl4 = 3.087(2) Å and N4···O5w = 2.743(6) Å. All details of these H-bonding interactions are tabulated in Table S1. In complex **2** the protonated receptor $[\mathbf{L}H_4]^{4+}$ slips from the face to a distant position and does not form any capsular assembly unlike the complex **1** which is illustrated in Fig. 3c**.** Each tripodal receptor interacts with the adjacent tripodal by several H-bonding interactions arising from N—H···Cl, N—H···Ow and Ow—H···Cl that generates the supramolecular structure. Close inspection in crystal structure shows three $[NH_3]^+$ groups of one $[\mathbf{L}H_4]^{4+}$ unit interacts with other two $[\mathbf{L}H_4]^{4+}$ unit *via* chloride-water bridge and such way they form non-capsular structure. The $[\mathbf{L}H_4]^{4+}$ units are linked each other by chloride-water [Cl_2-H_2O 'V' shaped] bridge, with the help of $[NH_3]^+$ groups form several fused cyclic rings (octamer, hexamer, pentamer and tetramer) shown in Fig. 3d. The packing diagram of complex **2** along *c*-axis shows that the hydrophilic layer of chloride-water channel propagate through cationic bilayer generated by protonated receptor (Fig. S21b). The weak interactions mainly comprising of aromatic C—H_{ar}···Cl and aliphatic C—H_{alp}···Cl are also involved in supramolecular assembly. The presence of H-bonded water molecule has also been confirmed by solid-state FT-IR analysis. The presence of a moderate broad signal at 3440 cm^{-1} in complex **2** is attributed to the stretching frequency of the water molecule which is absent in free receptor (Fig. S10). Additionally, the bulk phase purity of the complex **2** has been established by PXRD experiment (Fig. S16).

Structural Study of Complex [LH_4·4Cl](3)

The solid state structure of the chloride complex **3** displayed by X-ray analysis shows it crystallizes in highly symmetric hexagonal system of space group *R-3c* with crystallographically independent one third of the tetra-protonated receptor $[\mathbf{L}H_4]^{4+}$ and four chloride ions as asymmetric unit. In this case the complex does not contain any water of crystallization. All three arms are identical and apical N-atom possesses C_{3v} symmetry. The separation of N—C bond is 1.500 Å which confirmed the protonation on apical N-atom. The *endo*-oriented hydrogen atom interacts with all three ethereal oxygen and brings three arms closer by H-bonding (N1···O = 2.770 Å, Fig S22a). The ethereal bond distance (O···O = 3.575 Å) and torsion angle (N_{apical}–C–C–O_{ether} = 60°) value indicates the folded conformation. Similarly, three arms are posed each other vertically and form C_{ar}—H···π interactions that also stabilized bowl shaped conformation. All three hydrogen of $[NH_3]^+$ are engaged in H-bonding with three chloride ions of distances N2···Cl1 = 3.041(3) Å, N2···Cl2 = 3.184(4) Å and N2···Cl3 = 3.038(3) Å (Fig. S22b). Unlike hydrated chloride complex **2**, here, two $[\mathbf{L}H_4]^{4+}$ units meet face to face and bimolecular capsule is built which is explained by top view in Fig. 4a. In this case total six chloride ions are involved in capsule and

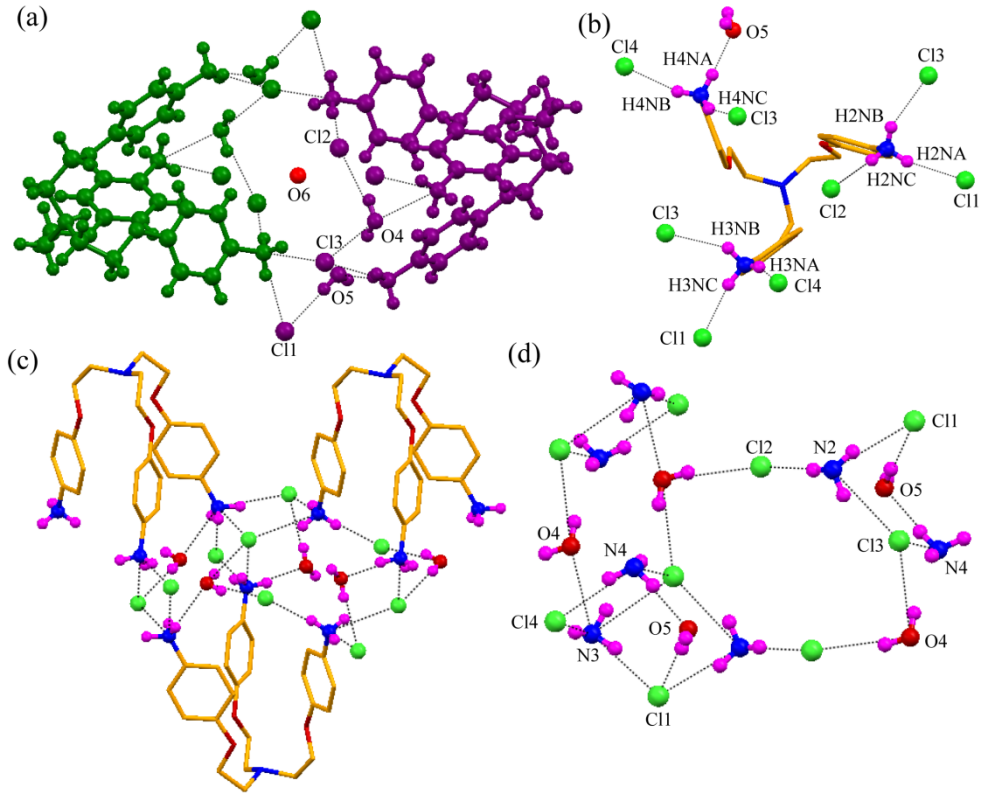

Fig. 3 (a) Color scheme showing the cetrosymmetric molecular structure having an inversion center with respect to O6w in complex **2**. (b) Showing coordination environment and H-bonding interactions of three $[NH_3^+]$ groups with chloride ions and water molecule. (c) Depicting non-capsular assembly and interaction of $[\mathbf{L}H_4]^{4+}$ with adjacent receptor mediated by chloride-water in complex **2**. (d) Perspective representation of 'V' shaped small $[Cl_2\text{-}H_2O]^{2-}$ cluster that form several cyclic rings with the help of $[NH_3^+]$ group in non-capsular assembly. H-atoms omitted from the pictures for clarity.

holds two $[\mathbf{L}H_4]^{4+}$ unit firmly through formation of chloride ion belt enriched with Cl···H—N H-bonding interactions with $[NH_3]^+$ groups which is depicted in Fig. 4b. Close view of H-bonding involved in the capsular assembly is shown in Fig. 4c. Detailed H-bonding parameters are given in Table S1. The distance between two vertical N-atoms in this capsule is dropped to 16.706 Å as compared to **1** presumably due to absence of water molecules in the capsular assembly. Each capsule attached with the adjacent capsule through the formation cyclic $[Cl^-\text{-}NH_3^+]$ motif highlighted in Fig. 4d. Crystal packing viewed along *c*-axis results star like assembly of the molecular capsules (Fig. S23a). The extended packing diagram along *a*-axis produced anionic channel surrounded by cationic bilayers (Fig. S23b). The IR spectrum of the dehydrated complex does not contain any peak in the region of 3400-3200 cm^{-1} indicating absence of water molecule as expected (Fig. S11). The complex remains in pure phase even in larger quantity as observed from similar simulated and experimental PXRD pattern (Fig. S17).

Structural Study of Complex $[LH_4{\cdot}4Br{\cdot}5H_2O](4)$

Single crystal X-ray shows the complex **4** crystallizes in commonly available monoclinic system of space group $P2_1/c$ with an asymmetric unit that contains one tetra-protonated $[\mathbf{L}H_4]^{4+}$, four bromide ions and five lattice water molecules. One bromide ion (Br3) lies on the C_{3v} symmetric apical N-atom. The N—C bond distance (1.505 Å) in complex **4** is ideal for apical nitrogen protonated receptor. The hydrogen on apical

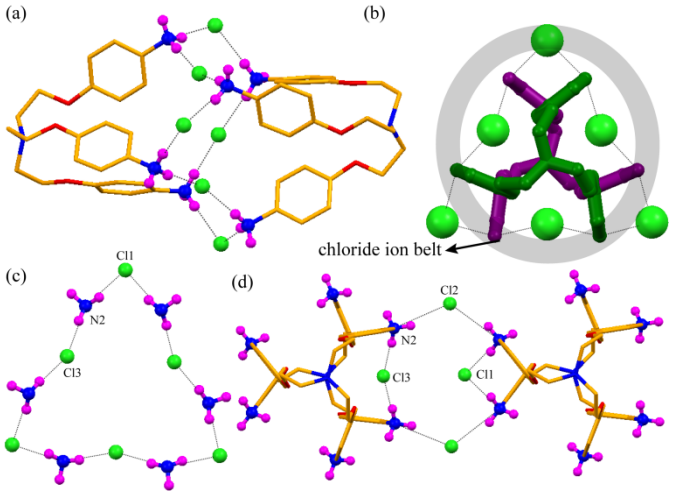

Fig. 4 (a) Side view depicting bimolecular capsular aggregate by chloride ions in complex **3**. (b) Top view showing bimolecular capsule stitched by chloride ion belt. (c) Partial structure showing the H-bonding in anion belt of the bimolecular capsule in complex **3**. (d) View depicting the interaction between two molecular capsules mediated by $[Cl^-\text{-}NH_3^+]$. H-atoms omitted from the pictures for clarity.

N-atom is *endo*-oriented and interacts with all three ethereal oxygen atoms (average N1···O = 2.774 Å, Fig. S25a). Bowl shaped cavity of hydrated bromide complex **4** like other complexes also established from ethereal bond distance (O···O

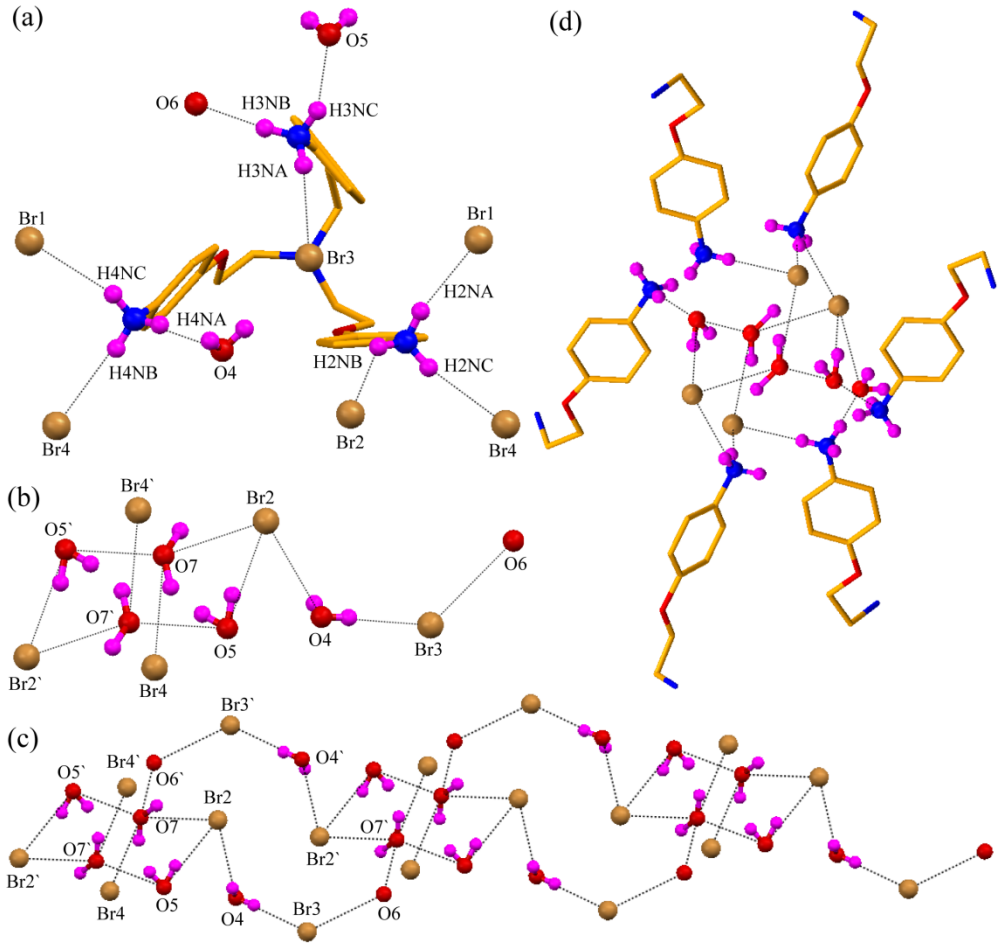

Fig. 5 (a) Showing coordination environment and H-bonding interaction of $[NH_3]^+$ groups with bromide ions and water molecules in complex **4**. (b) View depicting minimum repeating fragment of bromide-water cluster $[Br_5\text{-}(H_2O)_6]^{5-}$ containing hexameric chair $[Br_2\text{-}(H_2O)_4]^{2-}$. (c) Infinite array of bromide-water cluster in which two $[Br_5\text{-}(H_2O)_6]^{5-}$ met in an inversion center and formed fused decameric ring in complex **4**. (d) Partial structure depicting interaction of bromide-water hexamer with $[LH_4^+]$. H-atoms omitted from pictures for clarity.

= 3.597 Å) and torsion angle value (N_{apical}–C–C–O_{ether} = 62°). Three arms are connected each other by C—H_{ar}···π interactions and also holds the three arms together to stabilize bowl shape conformation. Fig. 5a explains the binding mode of three $[NH_3]^+$ groups with bromide ions and water molecules. Three hydrogen of $[N(2)H_3]^+$ donate all hydrogen to bind three bromide ions *via* three N2···Br1 = 3.225(5) Å, N2···Br2 = 3.291(5) Å and N2···Br4 = 3.321(5) Å H-bonds. The other $[N(3)H_3]^+$ is surrounded by one bromide ion and two water molecules having distances N3···Br3 = 3.415(5) Å, N3···O5w = 2.809(6) Å and N3···O6w = 2.782(7) Å. The third $[N(4)H_3]^+$ is involved in H-boding with two bromide ions and one water molecule having H-bonding parameters N4···Br1 = 3.344(5) Å, N4···Br4 = 3.388(5) Å and N4···O4w = 2.771(8) Å. All H-bonding details are given in Table S1. Crystal structure study shows the $[\mathbf{L}H_4]^{4+}$ units displaced from the face to a distant position in such a manner that they form non-capsular assembly like hydrated chloride complex **2** (Fig. S24). Each units are connected each other by $[Br^-\text{-}H_2O]$ linker enriched with several H-bonding. The most noteworthy feature of complex **4** is that we isolated very significant anion-water cluster composed of bromide ions and water molecules. We observed an unique anion-water cluster $[Br_5\text{-}(H_2O)_6]^{5-}$ having cyclic six membered ring $[Br_2\text{-}(H_2O)_4]^{2-}$ and tail $[Br\text{-}(H_2O)_2]^-$ which is illustrated in Fig. 5b. A careful analysis reveals that centrosymmetric cyclic hexamer composed of one bromide ions (Br2), two water molecules (O7w, O5w) and their centrosymmetric equivalents and resulted the formation of cyclohexane chair like conformation (Fig. S25c). The hybrid cyclic hexamer is quite similar to purely water hexamers found in several hydrated crystal systems[24] where bromide ion replaces the water molecule and persist the similar conformation (chair like). In the chair conformation four water molecules lies on the basal plane, two bromide are on above and below of the plane. In the hexamer two hydrogen of O5w is accepted by Br2 and O7w, whereas one hydrogen of O7w is accepted by Br2 giving a H-bonded motif $R_4^4(12)$. The H-bonding involved in cyclic hexamer are as follows; Br2···O5w = 3.362(6) Å, Br2···O7w = 3.267(7) Å and O5w···O7w = 2.805(9) Å. The Br···O and O···O separation in this hybrid water cluster is comparable to reported value observed in bromide-water clusters[14,18,25] and water hexamers.[24] Two type of bond angles found in cyclic hexamer *viz* ∠O5–Br2–O7 = 67.0(2)° and ∠O7–O5–Br2 = 110.4(2)° are ideal for tetrahedral water molecule which is frequently observed in hexagonal ice.[26] Other bond angles like ∠O–O–O, ∠O–O–Br, ∠Br–O–Br and ∠Br–Br–O existing outside of the

hexameric ring span the range of 64.0(1)-131.5(1)°. Detail structural scrutiny of hybrid bromide-water hexamer shows that it is bi-substituted at O7w and mono-substituted at Br2. O7w contains bromide ion (Br4) in axial and water molecule (O6w) in equatorial position, Br2 contains one water molecule (O4w) in axial position from where a tail of [O4w-Br3-O6w]$^{-}$ is extended. The tail along with hexamer meet each other at O7w of the next hexamer in a centrosymmetric fashion with perfect inversion center leading to the formation of fused decameric ring (with hexamer) and as a result extended polymeric chain of hybrid bromide-water cluster is obtained in the crystal lattice as shown in Fig. 5c. The decameric ring is also substituted at Br3 by [O8w-Br1]$^{-}$. The strong and medium H-bonds involved in decamer are Br2···O4w = 3.267(7) Å, Br3···O4w = 3.316(6) Å and Br3···O6w = 3.356(5) Å. In this cluster water molecules and bromide ions shows variety of coordination like four and three coordination with the help of protonated receptor. The coordination environment of bromide-water cluster [Br_5-$(H_2O)_6$]$^{5-}$ is depicted in Fig. 5d which clearly shows that several tripodal arms are involved in stabilization of the cluster through its [NH_3^+] end that form H-bonds with bromide ions and water molecules. Crystal packing along *b*-axis shows the propagation of hydrophilic bromide-water channel surrounded by cationic bilayer of the protonated receptor (Fig. S25b). In addition few other weak interactions like C9—H_{al}···Br1, C4—H_{ar}···Br4, C2—H···O7w and C10···Cg also helps for aggregation of the protonated receptor. We confirmed the presence water molecule in crystal lattice of hydrated bromide complex **4** by IR spectra and broad vibration frequency appears at 3435 cm^{-1} corresponding to O—H stretching vibration (Fig. S12). The bulk phase purity of the complex is also confirmed by PXRD study where simulated and experimental pattern coincide each other (Fig. S18).

Structural Study of Complex [4LH_4·16I·7H_2O](5)

The complex **5** crystallizes in triclinic system with a *P-1* space group. The asymmetric unit contains two crystallographic independent tetra-protonated receptor [$\mathbf{L}H_4$]$^+$ (N1 and N5 unit; naming according to the numbering of apical N-atom), eight iodide ions and four water of crystallization. Each protonated tripodal receptor in the asymmetric unit possesses C_{3v} symmetry passing through apical N-atom and an iodide ion (I1) lies on the C_{3v} symmetric apical N-atom in N1 unit. The average bond distance between apical N-atom and adjacent carbon atom are 1.508 Å and 1.513 Å in N1 and N5 unit respectively which suggested protonation on apical N-atom. The hydrogen atom on apical N-atom in both cases are *endo*-oriented and H-bonded in trifurcated fashion with ethereal oxygen atoms (average N1···O = 2.766 Å and N5···O = 2.770 Å, Fig. S26), which helps to bring three arms in closer distance. Structural analysis shows one arm stay away from the other two arms by a small margin and not able to form any C—H···π interaction with other two arms, hence we observed only one orthogonal C—H···π interaction in N5 unit, whereas in N1 unit we observed three C—H···π interactions falling in acceptable distances (Fig. S26). Though ethereal bond distance (O···O = 3.586 Å) and torsion angle value (N_{apical}–C–C–O_{ether} = 62°) suggest the bowl shaped conformation in both unit like all other complexes. The crystal structure shows that all six [NH_3]$^+$ group interacts with iodide ions and water molecules depicted in Fig. 6a and 6b. Coordination environments of [N(2)H_3]$^+$, [N(3)H_3]$^+$ and [N(6)H_3]$^+$ are same and each groups are surrounded by two iodide ions and one water molecule. On the other side each [N(4)H_3]$^+$ and [N(8)H_3]$^+$ are H-bonded with three and four iodide ions respectively. Only [N(7)H_3]$^+$ group interacts only with two iodide ions. All H-bonding interactions are summarized in Table S1. In iodide complex each tripodal unit displaced from the face and connected through iodide-water interactions to form non-capsular assembly like complex **2** and **4 (**Fig. S27). Solid state structure shows two symmetry independent tripodal receptor form two types of non-capsular aggregations with the help of H-bonding substances like iodide ions, water molecules and [NH_3]$^+$ groups. It is noteworthy to mention that we observed a well-defined discrete iodide-water cluster in non-capsular assembly formed by N5 unit. The iodide ion (I4) and two water molecules (O7w and O10w) formed 'V' shaped structure *via* I4···O10w = 3.630(3) Å and O7w···O10w = 2.830(4) Å H-bonding interactions. Such two 'V' shaped structures met each other through two oxygen end *via* O7w···O10w = 2.920(4) Å contact and led to the formation of iodide-water cluster [I_2-$(H_2O)_4$]$^{2-}$ containing cyclic water tetramer shown in Fig. 6c. The I···O separation observed in our study is comparable to the theoretically obtained value 3.67 Å.[9] The water tetramer in iodide-water cluster contains a perfect inversion center at the center of the square. The four water molecule lies on a plane and two iodide ions occupy above and below of the plane forming chair like conformation. Hence two iodide ions are inversely related with respect to inversion center in the tetramer. To the best possible placement of H-atoms in this cluster we noticed O7w donate its two hydrogen atoms towards two symmetric O10w and O10w presumably donates its two hydrogen to I4 ion. From the contribution of donor-acceptor properties of water molecules a cyclic water tetramer is formed with a H-bonding motif $R_4^2(8)$**.** Four H-atoms from two water molecules (O7w) are only involved in the formation of cyclic water tetramer and H-atoms of other two water molecules (O10w) are directed just outside of the ring. Such type of water tetramer is not so common and rarely observed in crystal lattice.[27] The discreet iodide-water cluster is surrounded by cationic tripodal and stabilized by several strong and weak H-bonding interactions shown pictorially in Fig. 6e. The water molecule O7w of tetramer accept two hydrogen from N6 and C42 of the tripodal receptor forming N6···O7w =2.780(3) Å and C42···O7w = 3.270(2) Å H-bonding. On the other hand, iodide ion (I4) interacts with its neighbored tripodal receptor *via* N7···I4 = 3.600(2) Å, N7···I4 = 3.650(1) Å and C41···I4 = 3.850(1) Å contacts. With the best of our knowledge structural study of iodide-water cluster is very less,[19] our report of iodide-water cluster [I_2-$(H_2O)_4$]$^{2-}$ in organic system has not been reported previously. So iodide-water cluster [I_2-$(H_2O)_4$]$^{2-}$ observed in organic receptor is unprecedented. Crystal packing motif of complex **5** as viewed down along *a*-axis showing the cationic bilayer assembly formation of cationic ligand moieties with the iodide-water channel being entrapped between the adjacent bilayers (Fig. S27c). The IR spectra of complex **5** indicate a broad band centered around 3420 cm^{-1} and that can be attributed to O-H stretching frequency suggesting presence of water molecule (Fig. S13). The bulk phase purity of the complex has also been confirmed by PXRD study where simulated and experimental pattern coincide each other (Fig. S19).

Thermal analysis of the complexes

Nature of water molecules in the crystal lattice and thermal stability of the halide complexes are examined by thermogravimetric analysis (TGA) and differential scanning calorimetry (DSC) experiments. The capsular and non-capsular

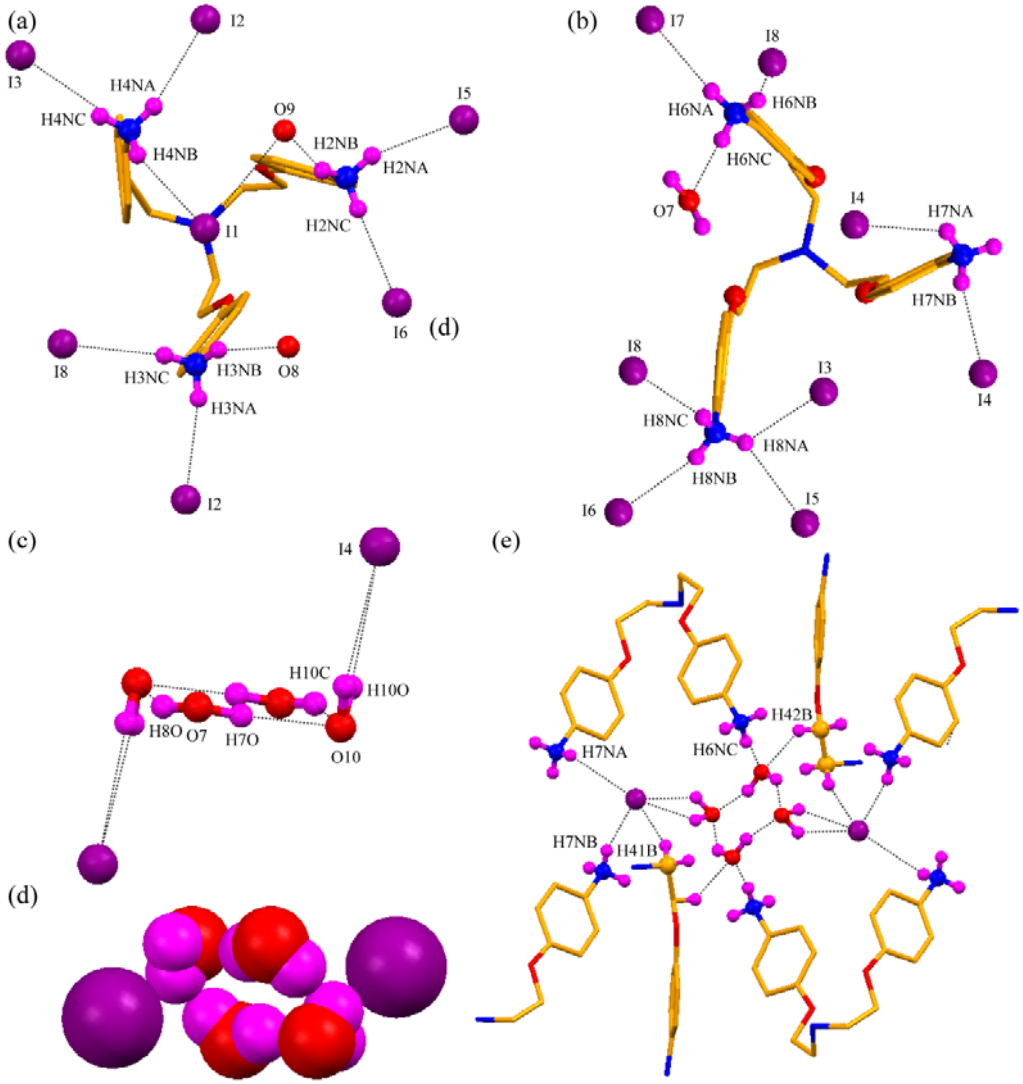

Fig. 6 (a) Depicting coordination environment and H-bonding interactions of the $[NH_3]^+$ groups of two symmetry independent $[LH_4]^+$ unit with iodide ions and water molecules in complex **5**. (b) Image showing iodide-water cluster $[I_2\text{-}(H_2O)_4]^{2-}$ having square arrangement of water tetramer in complex **4**. (c) Space fill model of $[I_2\text{-}(H_2O)_4]^{2-}$ cluster. (d) View describing interaction and stabilization $[I_2\text{-}(H_2O)_4]^{2-}$ cluster by cationic tripodal receptor.

assembled supramolecular structures are a consequence of anion-water and anion-water-receptor interactions. Their stabilities are well explained by thermal analysis (Fig. 7). The fluoride complex **1**, exhibited continuous weight loss (for water molecule) up to ~194 °C, there is a weight loss of 5.75% at ~104 °C, which matches very well with calculated value 6.07% corresponding to two water molecules. Partially dehydrated complex is stable up to ~135 °C and after this remaining three water molecules (found 8.45%; calcd. 9.01%) are lost and continue to ~194 °C along with the melting of the complex. In DSC clear endothermic peak is observed at ~97 °C and at ~188 °C corresponding to these weight losses (Fig. 7a). For the chloride complex **2**, removal of all water molecules (five crystalline water molecules) are observed in a single step, with the weight loss of 6.26% (calcd. 7.34%) at ~88 °C. The indication of this weight loss is also noticed from endothermic peak at ~84 °C in its DSC curve. The dehydrated complex is stable up to ~240 °C and started to melt after ~240 °C (Fig. 7b). On other hand the anhydrous chloride complex **3** did not show any weight loss in the range of ~30-256 °C as expected from its crystal structure (absence of lattice water molecule) and is stable up to ~256 °C before it melts. This result is also achieved by the appearance of a sharp endothermic peak at ~256 °C in its DSC plot (Fig. 7c). The bromide complex **4** started to degrade lattice water molecules early stages at ~76 °C, a weight loss 10.15% (calcd. 10.78%) relative to five water molecules. This is further confirmed by an endothermic peak at ~76 °C in its DSC curve. The dehydrated complex is stable up to ~285 °C and then started to melt with an appearance of a endothermic peak at ~280 °C (Fig. 7d). Removal of water molecules from the iodide complex **5** occurred in single step. A one step weight loss of 3.70% (calcd. 3.26%) at ~105 °C for seven water molecules is observed and confirmed an endothermic peak at ~105 °C in DSC curve. The dehydrated salt is stable up to ~288 °C. After this temperature complex started to melt and for which an endothermic peak is appeared at ~275 °C in DSC curve (Fig. 7e).

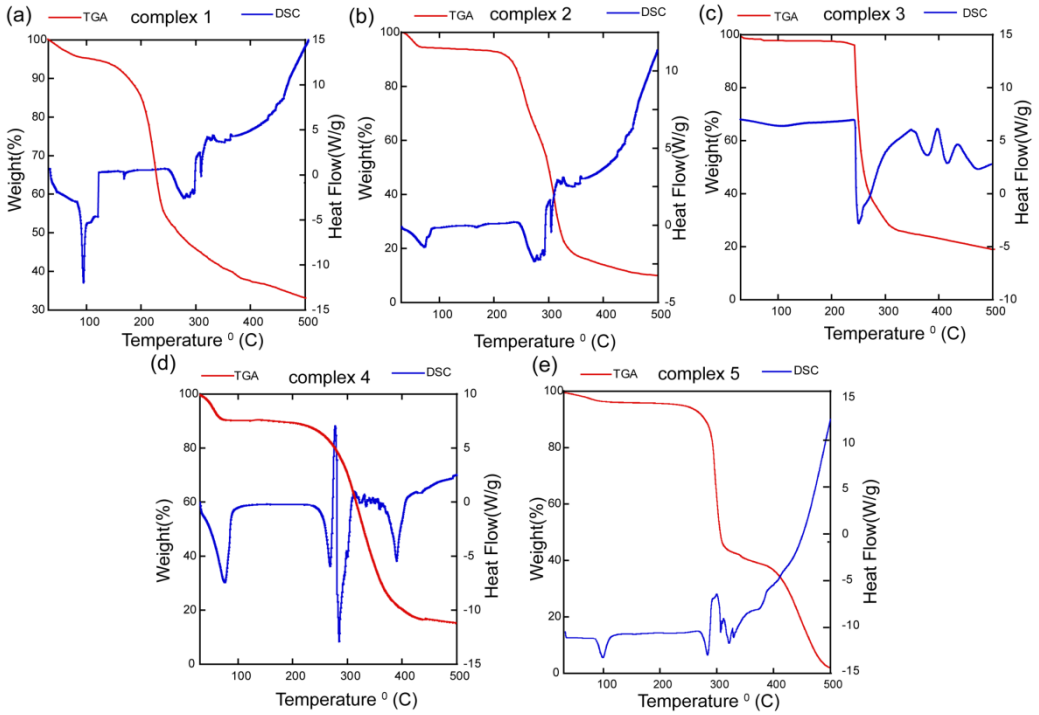

Fig. 7 Simultaneous curve of thermogravimetric analysis (TGA, red line) and differential scanning calorimetry (DSC, blue line) at the heating rate 7 °C/min for complexes **1-5**.

Conclusions

In summary, we have shown the capsular and non-capsular assembly of the cationic tripodal receptor by hydrophilic anion-water cluster. We established fluoride-water cluster and chloride ion belt mediated supramolecular assembly in bimolecular capsular fashion. On the other hand formation of non-capsular supramolecular association of the receptor is observed by chloride-water, bromide-water and iodide-water clusters. Moreover our observations underscore extended polymeric bromide-water cluster $[Br_5\text{-}(H_2O)_6]^{5-}$ having defined cyclohexane like chair conformation and discrete iodide-water cluster $[I_2\text{-}(H_2O)_4]^{2-}$ containing water tetramer in solid state. Existence of hydrophilic anion-water channels surrounded by cationic bilayers of tripodal receptor can elucidate the behavior of hydrated anionic species in confined environment. Our results would also help to exploit the complex hydration phenomena and anion-water interactions observed in physiology and hybrid anion-water clusters. These results may be helpful for understanding anion-water mediated assembly process, stability and transportation of anions in water-membrane interfaces.

Acknowledgements

G.D. acknowledges CSIR (01/2727/13/EMR-II) and SERB (SR/S1/OC-62/2011) New Delhi, India for financial support, CIF IITG and DST-FIST for providing instrument facilities. N.H. thanks IITG for fellowship.

Notes and references

[a]Department of Chemistry, Indian Institute of Technology Guwahati, Assam-781039, India. Fax: +91-361-2582349; Tel: +91-361-2582313; E-mail: gdas@iitg.ernet.in.

Electronic supplementary information (ESI) available: NMR spectra, IR spectra, simulated and experimental X-ray powder diffraction patterns, figures of the crystal structures and H-bonding table. For ESI and crystallographic data in CIF or other electronic format see DOI: 10.1039/b000000x/

References

1 (*a*) B. C. Faust, C. Anastasio, J. M. Allen and T. Arakaki, *Science*., 1993, **260**, 73; (*b*) S. Aime, M. Fasano, S. Paoletti, F. Cutruzzola, A. Desideri, M. Bolognesi, M. Rizzi and P. Ascenzi, *Biophys. J*., 1996, **70**, 482; (*c*) B. J. Finlayson-Pitts, *Anal Chem*., 2010, **82**, 770; (*d*) M. J. Molina and F. S Rowland, *Nature*., 1974, **29**, 810; (*e*) K. A. Prather, C. D. Hatch and V. H. Grassian, *Annu. Rev. Anal. Chem.,* 2008, **1**, 485; (*f*) D. Voet and J. G. Voet, *Biochemistry*., 2nd ed, John Wiley and Sons: New York, 1995; (*g*) P. Jungwirth and D. J. Tobias, *Chem. Rev.*, 2006, **106**, 1259; (h) K. S. Carslaw, T. Peter and S. L. Clegg, *Rev. Geophys.* 1997, **35**. 125.

2 (*a*) I. Benjamin, *J. Phys. Chem*., *B* 2010, **114**, 13358; (b) G. Niedner-Schatteburg and V. E. Bondybey, *Chem. Rev*., 2000, **100**, 4059; (*c*) B. L. Eggimann and J. I. Siepmann, *J. Phys. Chem*., *C* 2008, **112**, 210.

3 (*a*) M. Cametti and K. Rissanen, *Chem. Commun*., 2009, 2809; (*b*) M. A. Hossain, J. M. Llinares, S. M. P. Morehouse, D. Powell and K. Bowman-James, *Angew. Chem*., *Int. Ed*., 2002, **41**, 2335; (*c*) Q.-Q. Wang, V. W. Day and K. Bowman-James, *Angew. Chem*., *Int. Ed*., 2012, **51**, 2119; (*d*) P. S. Lakshminarayanan, E. Suresh and P. Ghosh, *Angew. Chem*., *Int. Ed*., 2006, **45**, 3807.

4 (*a*) E. K. Hoffmann, *Biochem. Biophys. Acta*., 1986, **864**, 1; (*b*) J. L. Sessler, P. A. Gale and W. S. Cho, *In Anion Receptor Chemistry* (Monographs in Supramolecular Chemistry); Ed.;

RSC: Cambridge, 2006; pp 1-413; (*c*) P. Zhou, F. Tian, J. Zou, Y. Ren, X. Liu and Z. Shang, *J. Phys. Chem., B* 2010, **114**, 15673; (*d*) F. Hofmeister, *Arch. Exp. Pathol. Pharmakol*., 1888, **24**, 247.

5 (*a*) Y. J. Marcus, J. Chem. Soc., Faraday Trans., 1991, 87, 2995; (*b*) A. Tongraar and B. M. Rode, *Phys. Chem. Chem. Phys*., 2003, **5**, 357.

6 S. Ayoob and A. K. Gupta, *Crit. Rev. Environ. Sci. Technol*., 2006, **36**, 433.

7 (*a*) R. Dutzler, E. B. Campbell, M. Cadene, B. T. Chait and R. MacKinnon, *Nature*., 2002, **415**, 287; (*b*) C. Miller, *Nature* 2006, **440**, 484.

8 (*a*) G. Rädlinger and K. G. Heumann, *Environ. Sci. Technol*., 2000, **34**, 3932; (*b*) R. W. Saunders, R. Kumar, S. M. MacDonald and J. M. C. Plane, *Environ. Sci. Technol*., 2012, **46**, 11854; (*c*) A. Saiz-Lopez, J. M. C. Plane, A. R. Baker, L. J. Carpenter, R. von Glasow, J. C. Gómez Martin, G. McFiggans and R. W. Saunders, *Chem. Rev*., 2012, **112**, 1773; (*d*) M. I. Guzman, R. R. Athalye and J. M. Rodriguez, *J. Phys. Chem*., A 2012, **116,** 5428.

9 H. M. Lee, D. Kim and K. S. J. Kim, *J. Chem. Phys.*, 2001, **114**, 4461.

10 M. Arunachalam and P. Ghosh, *Chem. Commun*., 2009, 5389.

11 M. Arunachalam and P. Ghosh, *Chem. Commun*., 2011, **47**, 6269.

12 M. A. Hossain, M. A. Saeed, A. Pramanik, B. M. Wong, S. A. Haque and D. R. Powell, *J. Am. Chem. Soc*., 2012, **134**, 11892.

13 R. Custelcean and M. G. Gorbunova, *J. Am. Chem. Soc*., 2005, **127**, 16362.

14 A. Basu and G. Das, *Chem. Commun*., 2013, **49**, 3997.

15 S. Chakraborty, R. Dutta, M. Arunachalam and P. Ghosh, *Dalton Trans*., 2014, **43**, 2061.

16 J. R. Butchard, O. J. Currnow, D. J. Garrett and R. G. A. R. Maclagan, *Angew. Chem., Int. Ed.*, 2006, **45**, 7550.

17 M. N. Hoque, A. Basu and G. Das, *Cryst. Growth Des*., 2012, **12**, 2153.

18 A. Bakhoda, H. R. Khavasi, and N. Safari, *Cryst. Growth Des*., 2011, **11**, 933.

19 W. Dong, Y. Ou-Yang, H.-B. Song, D.-Z. Liao, Z.-H. Jiang, S.-P. Yan and P. Cheng, *Inorg. Chem*., 2006, **45**, 1168.

20 (*a*) A. Pramanik, S. Majumdar and G. Das, *CrystEngComm*., 2010, **12**, 250; (*b*) M. N. Hoque, A. Basu and G. Das, *Cryst. Growth Des*., 2014, **14**, 6; (*c*) A. Gogoi and G. Das, *Cryst. Growth Des*., 2012, **12**, 4012; (*d*) M. N. Hoque, A. Basu and G. Das, *Supramol. Chem*. DOI 10.1080/ 10610278.2013.844811.

21 S. K. Dey and G. Das, *Cryst. Growth Des*., 2010, **10**, 754.

22 (*a*) G. M. Sheldrick, SAINT and *XPREP*, 5.1 ed.; Siemens Industrial Automation Inc.: Madison, WI, 1995. (*b*) *SADABS, empirical absorption Correction Program*; University of Göttingen: Göttingen, Germany, 1997. (*c*) G. M. Sheldrick, *SHELXTL Reference Manual: Version 5.1*; Bruker AXS: Madison, WI, 1997. (*d*) G. M. Sheldrick, *SHELXL-97: Program for Crystal Structure Refinement;* University of Göttingen: Göttingen, Germany, 1997**. (***e***)** Mercury 2.3 Supplied with Cambridge Structural Database; CCDC: Cambridge, U.K., 2012.

23 (*a*) S. K. Dey, A. Pramanik and G. Das, *CrystEngComm*., 2011, **13**, 1664; (*b*) S. K. Dey, B. Ojha and G. Das, *CrystEngComm*., 2011, **13**, 269; (*c*) P. Bose, I. Ravikumar and P. Ghosh, *Inorg. Chem*., 2011, **50**, 10693; (*d*) A. Danby, L. Seib, N. A. Alcock and K. Bowman-James, *Chem. Commun*., 2000, 973.

24 (*a*) T. Hu, X. Zhao, X. Hu, Y. Xu, D. Sun and D. Sun, *RSC Adv*., 2011, **1**, 1682; (*b*) S. Khullar and S. K. Mandal, *CrystEngComm*., 2013, **15**, 6652; (*c*) S. K. Ghosh and P. K. Bharadwaj, *Inorg. Chem*., 2004, **43**, 5180; (*d*) S. K. Ghosh and P. K. Bharadwaj, *Inorg. Chem*., 2003, **42**, 8250.

25 P. Manna, S. K. Seth, A. Bauzá, M. Mitra, S. R. Choudhury, A. Frontera and S. Mukhopadhyay, *Cryst. Growth Des*., 2014, **14**, 747.

26 D. Eisenberg and W. Kauzmann, *The Structure and Properties of Water*, Oxford University Press: Oxford, UK, 1969.

27 (*a*) S. pal, N. B. Sankaran and A. Samanta, *Angew. Chem., Int. Ed.*, 2003, **42**, 1741; (*b*) P. Yang, H.-Y. Zhou, K. Zhang and B.-H. Ye, *CrystEngComm*., 2011, **13**, 5658.

SYNOPSIS TOC

In this report we described capsular and non-capsular assembly of polyammonium tripodal receptor into supramolecular network driven by anion or anion-water cluster and solid state recognition of unique bromide-water $[Br_5\text{-}(H_2O)_6]^{5-}$ and iodide-water $[I_2\text{-}(H_2O)_4]^{2-}$ clusters.

.